

Comparison of the Properties of Leading and Trailing Sunspots

Yu. S. Zagainova^a, V. G. Fainshtein^b, and V. N. Obridko^a

^a Pushkov Institute of Terrestrial Magnetism, Ionosphere, and Radiowave Propagation, Russian Academy of Sciences (IZMIRAN), Troitsk, Moscow oblast, 142190 Russia

^b Institute of Solar–Terrestrial Physics, Siberian Branch, Russian Academy of Sciences, ul. Lermontova 126A, Irkutsk, 664033 Russia

e-mails: yuliazag@izmiran.ru; vfain@iszf.irk.ru; obridko@mail.ru

Received July 8, 2014

Abstract—The magnetic properties of leading and trailing sunspots were compared based on SDO/HMI and SDO/AIA data with a high spatial resolution for the growth phase and maximum of cycle 24. The properties of the solar atmosphere above sunspots are also discussed independently for both of these sunspot types. It was shown that the contrast in the He II 304 (C_{304}) line above the umbra of leading and single sunspots is on average smaller than such a contrast above the umbra of trailing sunspots and on average weakly depends on the umbra area for both C_{304} sunspot types. It was established that the minimal angle between the field direction and the normal to the solar surface at the field measurement site is smaller in leading sunspots than in trailing ones ($\alpha_{\min-ls} < \alpha_{\min-fs}$) in 84% of the considered magnetically connected “leading–trailing” sunspot pairs, and a positive correlation exists between angles $\alpha_{\min-ls}$ and $\alpha_{\min-fs}$. It was found that the C_{304} contrast increases with decreasing $\alpha_{\min-ls/fs}$ for leading and trailing sunspots, and the C_{304-ls}/C_{304-fs} ratio on average decreases with increasing $\alpha_{\min-ls}/\alpha_{\min-fs}$ ratio. The dependences of the maximal and average magnetic induction values in an umbra on the umbra area were constructed for the first time and compared independently for leading and trailing sunspots. It was concluded that the maximal and average magnetic field values do not vanish when the umbra area decreases to very small values. In all cases the magnetic field in leading and single sunspots is larger than in trailing ones.

DOI: 10.1134/S001679321406022X

1. INTRODUCTION

According to photospheric observations, sunspots are characterized by decreased values of the matter temperature and brightness and increased values of the magnetic field as compared to the remaining photospheric areas (Bray and Loughed, 1964; Obridko, 1985; Maltby, 1992). The Wolf number, i.e., the index of the sunspot number and groups simultaneously observed on the visible solar surface, is one of the most popular solar activity measures (Vitinsky et al., 1986).

Sunspots have been intensely studied from the beginning of their telescopic observations at the end of 1610. The first studies were mainly morphological. However, in the course of time, it became clear that sunspot origination and further evolution is a rather complex physical process, and the properties of single sunspots can substantially differ on the one hand and, on the other hand, are closely related to one another and to the surrounding solar areas in the subphotospheric layers and at different altitudes in the solar atmosphere (see, e.g., (Pipin and Kosovichev, 2011) and references therein).

Sunspots often form groups, in which spots with different properties can be distinguished; in this case a group itself has special characteristics governed by the set of all spots in a group. The westernmost sunspot in

a group, which has a larger area and is located closer to the equator as compared to the remaining sunspots in a group, is mostly called a leading or heading sunspot. Sunspots in a group of opposite field polarity are called tail or trailing sunspots. According to the Hale law on sunspot polarity in groups, “... in odd cycles the magnetic field of leading groups in the Northern Hemisphere has north-seeking polarity and that of trailing groups has south-seeking polarity. This pattern reverses its sign in the Southern Hemisphere and in going to an even cycle” (Obridko, 1985).

In the overwhelming majority of previous studies, sunspot properties were studied independently of their type: leading or trailing. The number of works comparing the properties of leading and trailing sunspots in one group and, on average, in many groups is relatively small. It was shown that there is almost no difference between the dependences of the contrast in the sunspot emission (Sobotka, 1986) and the photospheric magnetic field value in sunspots (Bray and Loughed, 1964) on the area of leading and trailing sunspots or the spot evolution stage. Gilman and Howard (1985) detected that the rotation velocities of leading and trailing sunspots slightly differ.

Recent studies have shown that the properties of leading and trailing sunspots actually pronouncedly differ according to their observations in different spec-

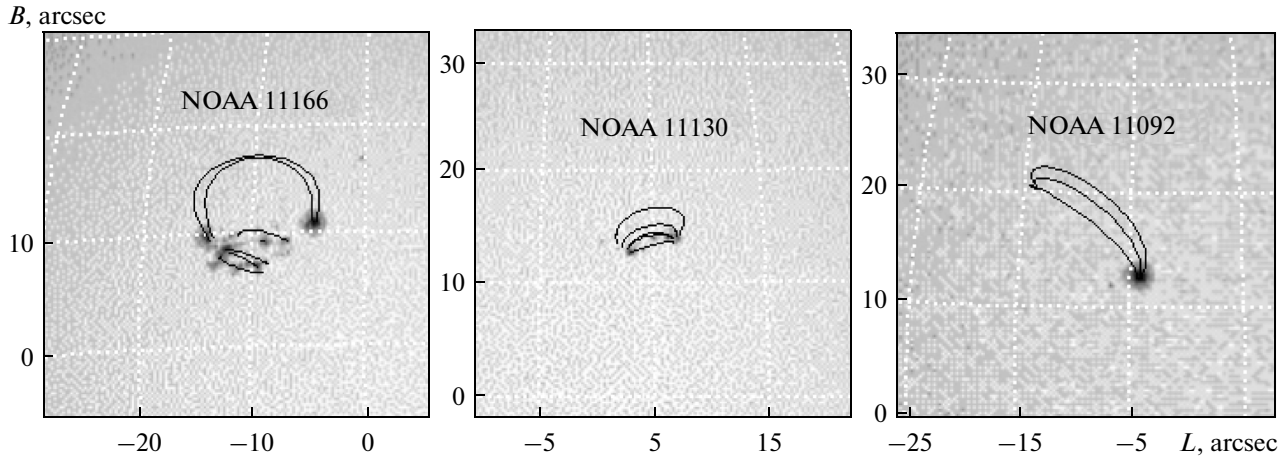


Fig. 1. Left: two large magnetically connected sunspots and new magnetically connected and independent smaller sunspots between them (March 8, 2011); center: a pair of small-scale magnetically connected sunspots (November 29, 2010); right: a single sunspot with the magnetic properties of a leading sunspot (August 3, 2010).

tral ranges. Thus, it was shown (Zagainova, 2011) that the dependences of the contrast in the He II 304 line and He I 10830 parameters of the IR triplet on the umbra area of leading and trailing sunspots substantially differ.

The magnetic properties of leading and trailing sunspots were also different. Using magnetic field calculations in a potential approximation based on Bd technology (Rudenko, 2001) and SDO data for 2010–2013, Zagainova et al. (2014) selected pairs of magnetically connected leading and trailing sunspots, the umbra of which are joined by magnetic field lines. It was found that the minimal angle between the field line and the normal to the solar surface (α_{\min}) in a leading sunspot is smaller than in a trailing one in $\sim 81\%$ of the cases. A positive correlation between the values of this angle in leading and trailing sunspots was revealed for the spots that satisfy this condition. It was shown that the dependence of angle α_{\min} on the umbra area differs in leading and trailing sunspots. A weak negative correlation was revealed between the α_{\min} angle and the maximal magnetic induction (B_{\max}) value in an umbra. In other words, field lines are on average more radial in magnetic tubes that form umbrae of leading and trailing sunspots and have stronger fields at the level of the photosphere.

Zagainova (2011) assumed that the difference in the magnetic field properties in an umbra of leading and trailing sunspots, which is characterized by the asymmetry of magnetic tubes connecting umbrae of two sunspot types, can result in increases in the He I atom layer optical depth in the 2^3S state and in the UV irradiance in $\lambda 304 \text{ \AA}$ above trailing sunspots as compared to leading ones. In turn, the difference of the He I 10830 IR triplet parameters from the leading and trailing sunspot umbra area can be explained by precisely this fact. This conclusion is based on the con-

cept of the ionization–recombination formation of the chromospheric helium IR triplet. Such a formation includes helium atom ionization by UV irradiance with the following transition of some atoms to the 2^3S metastable level after a certain delay, which is accompanied by the absorption of the photospheric continuum emission (Nikol’skaya, 1966; Livshits, 1975; Pozhalova, 1988). It was also indicated that the properties of single sunspots coincided with those of leading ones.

The present work continues the studies that were started in (Zagainova, 2011; Zagainova et al., 2014). The dependences of the contrast values in He II 304 above a C_{304} umbra on the umbra area of leading and trailing sunspots at the cycle 24 growth phase and maximum were compared based on the solar observations in the SDO/AIA 304 \AA channel (Lemen et al., 2012). The magnetic properties of leading and trailing sunspots, determined using the SDO/HMI magnetic field vector measurements with a high spatial resolution, were also compared for the same period.

2. DATA AND METHODS OF STUDIES

For analysis we selected the group of magnetically connected leading–trailing sunspot pairs that were observed in 2010–2013: the sunspots were connected by magnetic field lines calculated in the scope of the potential field–source surface model. Figure 1 from (Zagainova et al., 2014) illustrates magnetically connected sunspot pairs and a single sunspot. It turned out that magnetically connected sunspots were characterized by a distinct regular umbra with a circular or elliptical symmetry. In addition, we selected single sunspots with well-shaped umbra and penumbra for analysis. The list of the magnetically connected sunspot pairs selected for analysis is presented in Table 1, where the active region numbers, umbra areas, and

Table 1. List of magnetically connected sunspot pairs selected for analysis

1	2	3	4	5	1	2	3	4	5
Date	NOAA	S_L , MSH	S_F , MSH	N/S	Date	NOAA	S_L , MSH	S_F , MSH	N/S
Sept. 27, 2010	11109	51	10	N	Aug. 7, 2011	11266	3	4	N
Oct. 25, 2010	11117	15	22	N	Aug. 22, 2011	11272	4	2	S
		21	5	N			9	5	S
Nov. 29, 2010	11130	9	8	N	Oct. 15, 2011	11316	20	22	S
Jan. 4, 2011	11142	4	5	S		11319	8	3	N
Feb. 2, 2011	11150	7	7	S	Oct. 28, 2011	11330	68	7	N
Feb. 13, 2011	11158	12	12	S	Nov. 1, 2011	11334	15	2	N
		6	9	S	Nov. 7, 2011	11339	37	29	N
Feb. 14, 2011	11158	21	24	S		11338	24.5	8	S
Mar. 8, 2011	11166	30	21	N	Nov. 30, 2011	11361	18	10	N
Mar. 11, 2011	11169	22.5	8	N	Dec. 3, 2011	11365	7	4	N
Apr. 1, 2011	11183	19	5	N		11363	27	12	S
Apr. 3, 2011	11184	7	3	N	Dec. 5, 2011	11363	9	1	S
Apr. 13, 2011	11190	10	13	N		11364	61	14.5	N
Apr. 18, 2011	11193	21	4	N	Dec. 20, 2011	11382	23	3	S
Apr. 24, 2011	11195	30	23	S	Dec. 25, 2011	11384	71	8	N
May 5, 2011	11203	21	0.3	N	Jan. 20, 2012	11401	50	16	N
June 14, 2011	11234	3.3	1	S	Feb. 1, 2012	11413	15	7	N
July 30, 2011	11260	22	7.3	N	Feb. 11, 2012	11416	33	46	S
Aug. 1, 2011	11263	54	62	N	Feb. 20, 2012	11422	45	31	N
Aug. 3, 2011	11263	63	15.5	N					

With the date (column 1); active region number (column 2); umbra area (the areas of leading (S_L) and trailing (S_F) sunspots are given in columns 3 and 4, respectively); and magnetic field sign (column 5, N/S).

magnetic field signs are indicated. The data on single sunspots are combined in Table 2.

The SDO/AIA telescope has a spatial resolution of $\approx 0.5''$ (Lemen et al., 2011). The contrast in the $\lambda 304 \text{ \AA}$ line above an umbra was determined from the $C_{304} = I_S/I_0$ ratio, where I_S and I_0 are the intensity readings in the umbra and in the quiet area, respectively (for more detail, see (Zagainova, 2011)). The umbra area, expressed in millionths of the solar hemisphere (MSH), was found based on the sunspot images in continuum according to SDO/HMI data.

The present work analyzed the magnetic field characteristics in an umbra, such as the minimal angle (α_{\min}) between the field direction and the normal to the solar surface at the field measurement point and the maximal (B_{\max}) and average ($\langle B \rangle$) values of magnetic induction. To analyze the magnetic field properties in an umbra, we used the HMI vector magnetic field measurements (<http://hmi.stanford.edu/>), which make it possible to determine the magnetic induction (B), magnetic field vector inclination with respect to the angle of sight (δ), and azimuth (ψ), which is counted off counterclockwise in the sky plane from the

CCD matrix pixel column to the (transverse) magnetic field vector projection onto this plane. When the magnetic field is measured with HMI, the spatial resolution is $0.5''$. Solar images with the δ and ψ distributions are obtained only several times a day. When the field vector characteristics are determined, the problem of uncertainty is solved when the transverse field direction is found.

In our work we analyzed angle α between the field direction and the normal to the solar surface at a point where the magnetic field is measured. To find this angle based on the measured δ and ψ values, we obtained the relationships between angles α , δ , and ψ . The calculations were performed in the Cartesian coordinate system $[X, Y, Z]$ with the origin at the solar center, where the $0X$ and $0Y$ axes are in the equatorial plane, the $0Y$ and $0Z$ axes are in the sky plane, and the $0Z$ axis crosses the North Pole (we neglect the ecliptic plane inclination with respect to the equatorial plane). The $0X$ axis is directed along the line of sight and is perpendicular to the sky plane. We considered that the line of sight is perpendicular to the sky plane at all points within the solar disk. We introduced unit vectors \mathbf{b} and \mathbf{r} , which are directed along the field magnetic

Table 2. List of single sunspots selected for analysis

1	2	3	4	1	2	3	4
Date	NOAA	S , MSH	N/S	Date	NOAA	S_L , MSH	N/S
July 2, 2010	11084	23	S	May 22, 2011	11216	16	S
Aug. 3, 2010	11092	42	N	June 7, 2011	11232	12	N
Aug. 9, 2010	11093	25	N	July 17, 2011	11251	18	N
Sept. 21, 2010	11108	48	S	Oct. 8, 2011	11309	18	N
Oct. 19, 2010	11113	22	N	Oct. 10, 2011	11312	48	N
Oct. 19, 2010	11115	29	S		11309	14	N
Oct. 20, 2010	11113	21	N	Nov. 12, 2011	11340	17	S
Oct. 20, 2010	11115	25	S		11342	30	N
Nov. 22, 2010	11127	15	N		11341	18	N
Dec. 8, 2010	11131	73	N		11343	28	N
Dec. 9, 2010	11131	64	N	Nov. 17, 2011	11346	15	S
Jan. 5, 2011	11140	28	N	Nov. 24, 2011	11355	23	N
Mar. 30, 2011	11180	6	N	Nov. 26, 2011	11360	19	N
Apr. 10, 2011	11185	4	N				

With the date (column 1); active region number (column 2); umbra area (column 3, S); and magnetic field sign (column 4, N/S)

induction and along the upward normal to the solar surface at a point where the field is measured. The required angle (α) is the angle between vectors \mathbf{b} and \mathbf{r} . We used the expression for the scalar product of these vectors. We also bore in mind that the \mathbf{b} and \mathbf{r} lengths are equal to unity. Angle α between the magnetic field direction and the normal to the solar surface was found from the following relationship:

$$\begin{aligned} \cos(\alpha) &= \mathbf{b}_X \mathbf{r}_X + \mathbf{b}_Y \mathbf{r}_Y + \mathbf{b}_Z \mathbf{r}_Z \\ &= \cos(\theta') \cos(\varphi') \cos(\theta) \cos(\varphi) \\ &+ \cos(\theta') \sin(\varphi') \cos(\theta) \sin(\varphi) + \sin(\theta') \sin(\theta). \end{aligned} \quad (1)$$

Here θ is the vector \mathbf{r} latitude (i.e., the inclination of this vector to the equatorial plane); θ' is the vector \mathbf{b} latitude, $\theta, \theta' = [-90^\circ, 90^\circ]$; φ is the vector \mathbf{r} longitude (the angle counted off clockwise from the X axis in the equatorial plane to the vector \mathbf{r} projection onto this plane); φ' is the vector \mathbf{b} longitude, $\varphi = [0^\circ, 90^\circ] \cup [270^\circ, 360^\circ]$, $\varphi' = [0^\circ, 360^\circ]$ west of the central meridian; $\mathbf{b}_X, \mathbf{r}_X; \mathbf{b}_Y, \mathbf{r}_Y; \mathbf{b}_Z, \mathbf{r}_Z$ are the projections of vectors \mathbf{b} and \mathbf{r} onto the X , Y , and Z axes, respectively. Angle δ between \mathbf{b} and the $0X$ axis, which is determined from the SDO data ($\delta = [0^\circ, 180^\circ]$), and angle ψ between the Z axis and the projection of \mathbf{b} onto the YZ plane (the azimuth according to the SDO data, $\psi = [0^\circ, 360^\circ]$, counted off counterclockwise from the $0Z$ axis) are specified.

$$\sin(\theta') = \pm \sqrt{(1 - A^2)/(1 + B^2)}, \quad (2)$$

where $A = \cos(\delta)$; $B = -\tan(\psi) = \cos(\theta') \sin(\varphi')/\sin(\theta')$. Sign “+” corresponds to $\psi = [0^\circ, 90^\circ]$ or $[270^\circ, 360^\circ]$; sign “-”, to $\psi = [90^\circ, 270^\circ]$.

$$\cos(\theta') = \sqrt{(A^2 + B^2)/(1 + B^2)}, \quad \theta' = [-90^\circ, 90^\circ], \quad (3)$$

where $\theta' \geq 0$, if $\psi = [0^\circ, 90^\circ]$ or $[270^\circ, 360^\circ]$, and $\theta' < 0$ if $\psi = [90^\circ, 270^\circ]$.

$$\sin(\varphi') = \pm \sqrt{B^2(1 - A^2)/(B^2 + A^2)}, \quad (4)$$

where sign is “+” if $\psi = [180^\circ, 360^\circ]$ and “-” if $\psi = [0^\circ, 180^\circ]$.

$$\cos(\varphi') = \pm \sqrt{A^2(1 + B^2)/(A^2 + B^2)}, \quad (5)$$

where sign is “+” if $\psi = [180^\circ, 360^\circ]$, and “-” if $\psi = [0^\circ, 180^\circ]$.

Note that angle α was larger than 90° for magnetic field of negative polarity (the field vector is directed toward the Sun), and we subtracted the obtained α values from 180° in order to compare this angle with the angles for the field of positive polarity.

3. RESULTS

3.1. Comparison of the Emission Contrast in the Helium $\lambda 304 \text{ \AA}$ Line in Leading and Trailing Sunspots at the Cycle 24 Growth Phase and Maximum

It was shown (Zagainova, 2011) that the contrast in $\lambda 304 \text{ \AA}$ above an umbra of leading (C_{304-ls}) and single

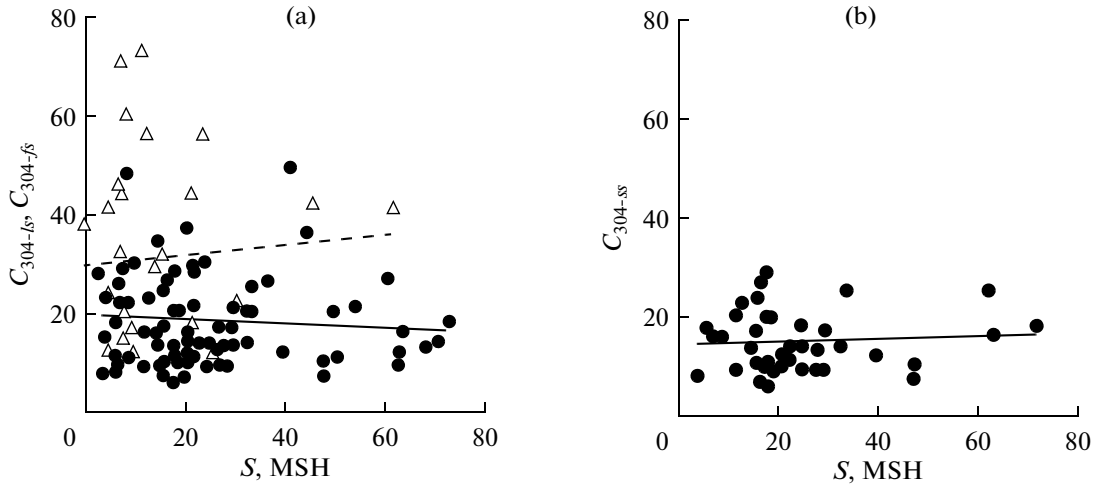


Fig. 2. Contrast in the He II 304 line above an umbra depending on the sunspot area: (a) for leading and single sunspots (circles) and trailing sunspots (triangles); (b) for single sunspots. The regression lines are shown by straight lines.

(C_{304-ss}), as well as trailing (C_{304-fs}), sunspots on average slightly changes with increasing S for an area of $S \approx 5$ MSH during the cycle 23 decline phase in 2002–2007. However, the contrast value in helium differs for leading and trailing sunspots. The average contrast value in the He II 304 line was $\langle C_{304-ss}, C_{304-fs} \rangle = 5 \pm 0.67$ according to the SOHO/EIT data ($\langle C_{304-ss}, C_{304-fs} \rangle \approx 7.5$ according to the CORONAS-F spacecraft data) for leading and single sunspots and $\langle C_{304-fs} \rangle = 12 \pm 2.52$ for trailing sunspots (the contrast value in $\lambda 304 \text{ \AA}$ on the regression line is presented here). For pores and small sunspots with a degenerate penumbra and an area smaller than 10 MSH, the contrast value in helium varied from 6 to 14.5.

Figure 2 shows the C_{304-ss} , C_{304-fs} , and C_{304-ss} values obtained according to the SDO/AIA data for the cycle 24 growth phase and maximum in 2010–2013. As in (Zagainova, 2011), the C_{304-ss} and C_{304-fs} values are combined in one group. But small sunspots and pores ($S < 10$ MSH), which had a developed umbra with circular or close to circular symmetry, were included in this plot as against (Zagainova, 2011). It is clear that the contrast in $\lambda 304 \text{ \AA}$ above an umbra of leading/single and trailing sunspots differs, and its value slightly varies depending on the area (S) in both cases. The contrast in $\lambda 304 \text{ \AA}$ varies from 8 to 50 above an umbra of leading sunspots/pores with a small area ($S < 10$ MSH) and from 12 to 71 for trailing sunspots. Only for single sunspots of leading polarity were contrasts C_{304-ss} and C_{304-fs} in these sunspots comparable with contrast C_{304-ss} for trailing sunspots.

Note that the average contrast value in $\lambda 304 \text{ \AA}$ for two sunspot groups was pronouncedly larger than in (Zagainova, 2011). According to the SDO data, $\langle C_{304-ss}, C_{304-fs} \rangle \approx 20$, $\langle C_{304-fs} \rangle \approx 32$ for sunspots $S =$

20 MSH. Such a difference is possibly related to the fact that the sunspot contrast was found using different instruments in two works. However, the contrast in helium above leading and single sunspots according to the CORONAS-F data during the same period was close to the values determined based on the SOHO/EIT data and differs by not more than a factor of ~ 1.5 as compared to the EIT data. The CORONAS-F spatial resolution is 1 pixel = 5.47 arcsec, which is twice as small as the SOHO/EIT spatial resolution (1 pixel = 2.63 arcsec). On the other hand, this work presents the results for the cycle 24 growth phase and maximum, which are characterized by different anomalous characteristics: small cycle height, substantially smaller magnetic fields, etc. (Akhmetov et al., 2014), whereas the results presented in (Zagainova, 2011) correspond to the decline phase of cycle 23. The C_{304} contrast values for sunspots in cycle 24 could also be anomalous.

Figure 2b presents the contrast values in the helium line for single sunspots depending on their area. In Fig. 2 we omit C_{304} for sunspots with anomalously large ($B > 3000$ G) magnetic field values. In contrast to leading sunspots, relatively large contrast values in $\lambda 304 \text{ \AA}$ are absent for single sunspots. The C_{304-ss} value was on average smaller by $\sim 30\%$ than the value for the combined data for leading and single sunspots.

3.2. Comparison of Magnetic Properties of Leading and Trailing Sunspots during the Cycle 24 Growth Phase

Using the SDO/HMI vector measurements of the magnetic field, we determined and compared the magnetic field properties in an umbra of leading and trailing sunspots. These measurements have substantially higher spatial resolution than the resolution provided by the magnetic field calculations in the solar atmosphere in a potential approximation, the data of

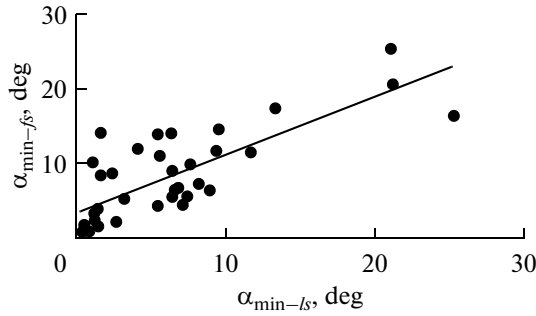


Fig. 3. Relation between the minimal angles between the magnetic field direction and the normal to the solar surface in an umbra of leading ($\alpha_{\min-ls}$) and trailing ($\alpha_{\min-fs}$) sunspots. The correlation coefficient is $k = 0.774$.

which were used to perform a similar analysis of the field properties in leading and trailing sunspots in our previous work (Zagainova et al., 2014).

We start analyzing magnetic field properties in an umbra with minimal values of the angle (α_{\min}) between the magnetic field direction and the normal to the solar surface at a point where the magnetic field was measured. Recall that the measured angle (α_{meas}) between the field direction and the radial direction is more than 90° when field polarity is negative (the sunward magnetic field vector); in this case $\alpha_{\min} = 180^\circ - \alpha_{\text{meas}}$. It turned out that the minimal angle between the field direction and the normal to the solar surface in leading sunspots was smaller than the angle in trailing sunspots in 84% of the considered pairs. For sunspots satisfying this condition, the average α_{\min} value was $\langle \alpha_{\min-ls} \rangle \approx 6.12^\circ$ in leading sunspots, $\langle \alpha_{\min-fs} \rangle \approx 16^\circ$, and $\langle \alpha_{\min-ls} / \alpha_{\min-fs} \rangle \approx 0.422$. All of these values are smaller than the corresponding values obtained when the magnetic field was calculated in a potential approximation (Zagainova et al., 2014). Figure 3 shows that a positive correlation with a correlation coefficient of 0.774 exists between the $\alpha_{\min-ls}$ and $\alpha_{\min-fs}$ values, for which $\alpha_{\min-ls} \leq \alpha_{\min-fs}$.

As in (Zagainova et al., 2014), a weak negative correlation between $\alpha_{\min-ls}$ and $\alpha_{\min-fs}$ on the one hand and between the maximal magnetic induction value (B_{\max}) and the umbra area (S) on the other hand was established based on SDO/HMI data. The correlation is almost absent for the $\alpha_{\min-fs}(S)$ dependence.

We omit the corresponding pots and only present the regression line equations, with indication of the correlation coefficient. For leading sunspots, the dependence of the minimal angle on the magnetic field maximal value is $\alpha_{\min-ls}(B_{\max}) = -0.00438B_{\max} + 16.223$, and the correlation coefficient is $k = -0.309$. For trailing sunspots, $\alpha_{\min-fs}(B_{\max-F}) = -0.0057B_{\max} + 27.437$, and $k = -0.157$. For leading sunspots, the angle value depending on area S is $\alpha_{\min-ls}(S) = -0.376 \pm 25.36$ (the correlation coefficient $k = -0.119$); for

trailing sunspots ($\alpha_{\min-fs}$), the regression line is almost parallel to the abscissa. These dependences were constructed for sunspots for which the $\alpha_{\min-ls} < \alpha_{\min-fs}$ condition was satisfied.

We also compared the magnetic field value (B_{\max}) in an umbra of leading and trailing sunspots with the umbra area (S) of these sunspots (see Fig. 4). The dependence of the magnetic induction value in an umbra on the umbra area (S) was discussed in several works (see the review in the monograph (Bray and Loughed, 1964)) and was summarized in (Ringnes and Jensen, 1960). Based on the results of several works, it was concluded that the relation between the magnetic induction (B) maximum and the area (S) agrees with the empirical relationship obtained in (Houtgast and van Sluiter, 1948) $B = 3700S/(S + 66)$; here B and S are measured in Gauss and millionths of visible hemisphere. The relation between the magnetic induction (B) maximum and the sunspot area (S) was also studied based on the magnetic field vector measurements in sunspots (Jin et al., 2006). It was shown that a logarithmic dependence exists between the field maximum in the umbra upper layers and the umbra area. However, leading and trailing sunspots were not separated in all studies of the $B-S$ dependence.

The Houtgast and van Sluiter formula, derived in 1948, contains a very important disadvantage. According to this formula, the sunspot magnetic field vanishes when the sunspot area tends toward zero. This formula reflects an early period in sunspot studies, when it was assumed that the magnetic field is absent outside sunspots and varies from 4000 G in large sunspots to 100 G in the smallest ones (Ringnes and Jensen, 1960). However, as the observation quality increased, it became clear that magnetic fields are rather large even in small sunspots. Steshenko (1967), Bumba (1967), and Beckers and Schroter (1968) indicated that the field in the smallest pores is not smaller than 1200 G and is even sometimes larger than 1800 G (Baranov, 1974). Antalova (1991) and Solov'ev and Kirichek (2014) also criticized this disadvantage of the Houtgast and van Sluiter formula.

At approximately the same time (in the 1960s), there appeared the concept of “kilogaussian tubes” (Sheeley, 1966, 1967; Harvey, 1971; Harvey and Livingston, 1969; Livingston and Harvey, 1969; Stenflo, 1973), according to which very small formations with a strength reaching 2000 G can exist.

At the same time, the Houtgast and van Sluiter formula expresses a very important property: saturation is formed at a certain instant, and the dependence of the magnetic field on the area becomes strongly weaker.

Figure 4 presents the magnetic field dependences on the area for leading ($B_{\max-L}, B_{\text{mean-L}}$) and trailing ($B_{\max-F}, B_{\text{mean-F}}$) sunspots and the formulas approxi-

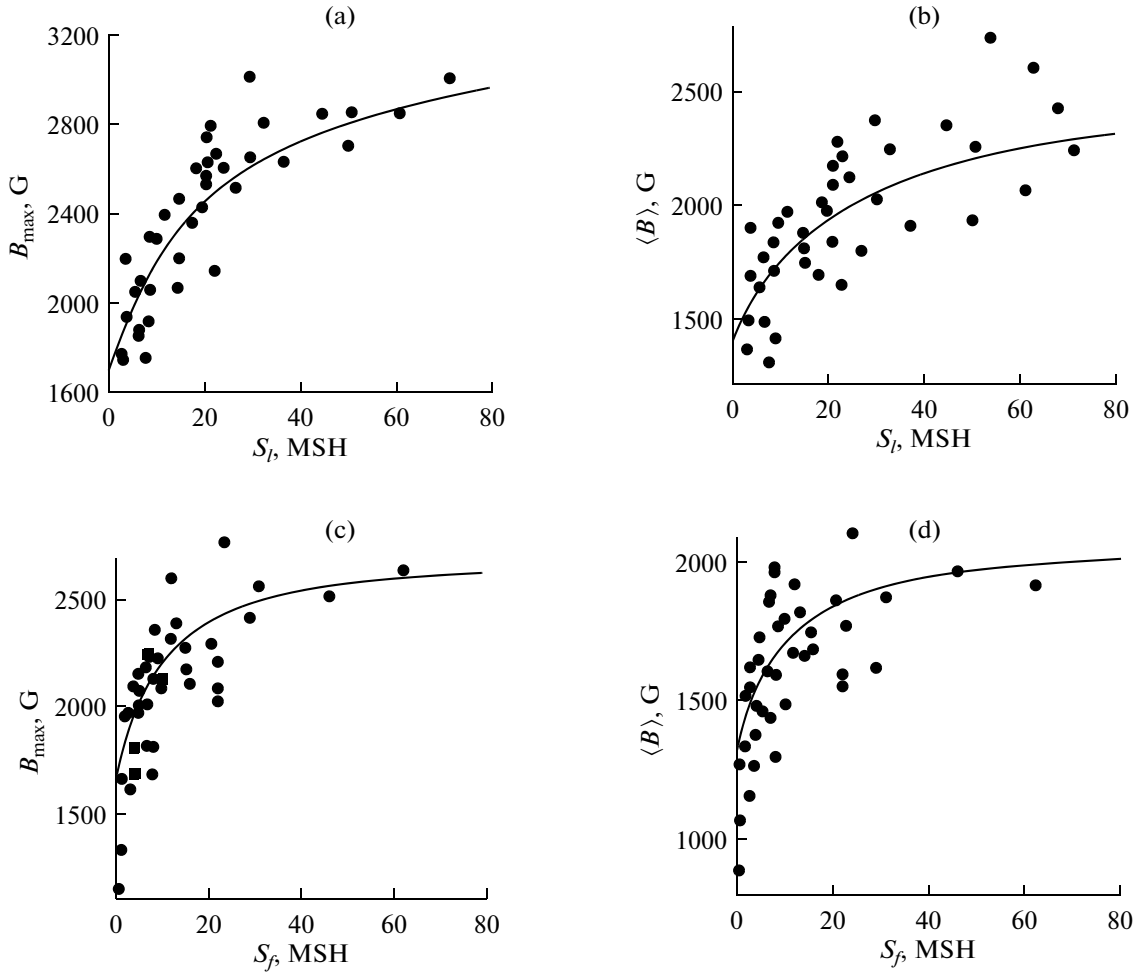


Fig. 4. The magnetic field value depending on the sunspot area: (a) the field maximal value for leading sunspots $B_{\max-L}(S_L) = 1700 + 1650S/(S + 25)$; (b) the average magnetic field value for leading sunspots $\langle B \rangle_L(S_L) = 1400 + 1400S/(S + 25)$; (c) the maximal magnetic field value for trailing sunspots $B_{\max-F}(S_F) = 1650 + 1100S/(S + 10)$; (d) the average field value for trailing sunspots $\langle B \rangle_F(S_F) = 1300 + 800S/(S + 10)$.

imating these dependences. The plots and approximating formulas shown in Fig. 4 indicate the following.

(i) Neither maximal nor mean magnetic field values vanish when the area decreases to very small values.

(ii) In all cases the magnetic field in leading and single sunspots is smaller than in trailing ones.

(iii) The threshold area value, when the curves start saturating, is of great importance. In the Houtgast and van Sluiter's formula, this value was 66 MSH and corresponded to a sunspot with a radius of ~ 8000 km. Our approximation gives threshold area values of ~ 25 and ~ 10 MSH for leading and trailing sunspots, respectively. This corresponds to radii of 5000 and 3100 km. We can conditionally consider that saturation is formed when the radius is comparable with the sunspot depth. The values obtained by us generally agree with the estimates made by Solov'ev and Kirichek (Solov'ev and Kirichek, 2014) and support the concept of a "shallow sunspot" developed by these

researchers. At such an interpretation, our data shows that trailing sunspots not only have a smaller magnetic field but are also potentially shallower formations.

(iv) Asymptotic values for a very large area are 3550 G for leading sunspots and 2750 G for trailing ones, and the smallest values can be ~ 1000 G.

We also analyzed the magnetic properties of well-shaped single sunspots with clearly defined umbra and penumbra. For these sunspots, the mean value of the minimal angle between the magnetic field direction and the direction along the positive normal to the solar surface is $\langle \alpha_{\min-ss} \rangle = 5.79^\circ$, $\langle B_{\max} \rangle \approx 2736$ G. In this case the average area of such sunspots is $\langle S \rangle \approx 24.64$ MSH, and the average contrast in $\lambda 304 \text{ \AA}$ in an umbra of such sunspots was $\langle C_{304} \rangle \approx 14.7$. This means that single sunspots selected for analysis are characterized by smaller α_{\min} values as compared to leading sunspots, which slightly differs from the contrast in helium, but by large

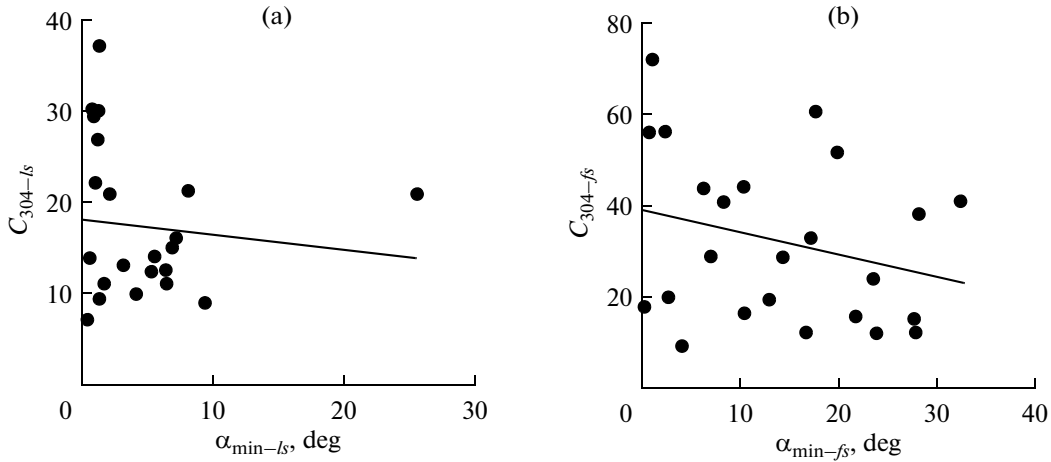


Fig. 5. Contrast C_{304} depending on the minimal angle (α_{\min}) between the magnetic field direction and the normal to the solar surface at the point where the field is measured for (a) leading and (b) trailing sunspots.

magnetic field values and a larger umbra area. This is confirmed by the conclusion that sunspots with stronger magnetic fields in their umbrae and smaller areas are on average characterized by smaller minimal angles α_{\min} . The relation of the minimal angle in single sunspots ($\alpha_{\min-ss}$) to the maximal magnetic induction (B_{\max}), as well to the area (S) and contrast in the helium line (C_{304}), is almost absent, or a weak negative correlation exists between these parameters. The absence of a relationship between $\alpha_{\min-ss}$ and B_{\max} and S apparently results from the fact that the number of single sunspots and sunspots with very small and very large B_{\max} and S values is very small in the sample. We also note one more result, which was achieved at the limit of statistical significance and requires larger samples for its confirmation. It turned out that angle $\langle \alpha_{\min-ss} \rangle_N = 6.45^\circ$ for sunspots of north-seeking polarity is larger than

the angle for sunspots of south-seeking polarity ($\langle \alpha_{\min-ss} \rangle_S = 4.35^\circ$).

3.3. Relation between Contrast in the 304 Å Line and Magnetic Properties of Leading and Trailing Sunspots

Our analysis indicated that a negative correlation exists between $\alpha_{\min-ls}$ and the contrast in $\lambda 304 \text{ \AA}$ above umbrae of leading sunspots (C_{304-ls}), as well as between $\alpha_{\min-fs}$ and C_{304-fs} in trailing sunspots (Fig. 5). These dependences and the plot in Fig. 6 were constructed for sunspots for which $\alpha_{\min-ls} \leq \alpha_{\min-fs}$ and, simultaneously, $C_{304-ls} \leq C_{304-fs}$. The dependences shown in Fig. 5 show that the contrast in $\lambda 304 \text{ \AA}$ on average increases with a decreasing minimal angle between the magnetic field direction and the positive normal to the solar surface at a point where the field is measured for leading/single and trailing sunspots. At the same time, the character of the relation between α_{\min} and C_{304} for leading and trailing sunspots differs (see Fig. 6): as the ratio of minimal angles in leading and trailing sunspots increases, the contrast ratio in an umbra of these sunspots increases. The dependences shown in Figs. 5 and 6 can be interpreted as follows: the magnetic field line configuration in sunspot groups is such that the amount of He II ions emitting in $\lambda 304 \text{ \AA}$ above an umbra of trailing sunspots is larger than such an amount above an umbra of leading sunspots.

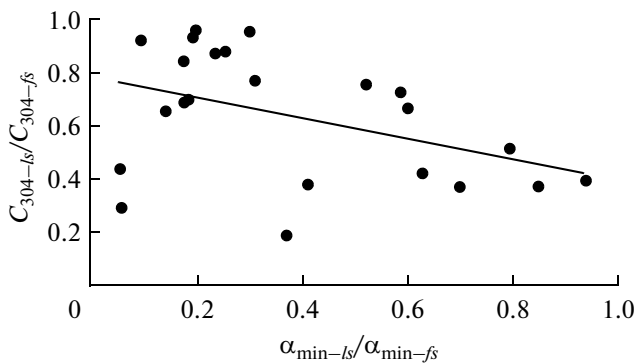


Fig. 6. Ratio of the contrast in the $\lambda 304 \text{ \AA}$ line for leading and trailing sunspots (C_{304-ls}/C_{304-fs}) depending on the ratio of the minimal angles in an umbra of two-type sunspots ($\alpha_{\min-ls}/\alpha_{\min-fs}$). The correlation coefficient is $k = -0.427$.

Figure 7 illustrates the dependence of the contrast in helium of leading and trailing sunspots on the maximal magnetic induction (B_{\max}) in an umbra. It is evident that $\langle C_{304-ls} \rangle(B_{\max})$ and $\langle C_{304-fs} \rangle(B_{\max})$ on average slightly vary when B_{\max} increases, as does the dependence on the sunspot area (see Fig. 1).

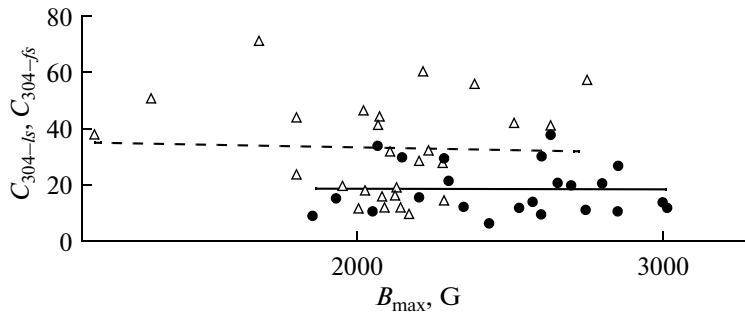


Fig. 7. Contrast in the $\lambda 304 \text{ \AA}$ line above an umbra of leading ($C_{304-\lambda s}$, circles) and trailing ($C_{304-\lambda s}$, triangles) sunspots depending on the maximal magnetic field value in an umbra of these sunspots (B_{\max}).

4. CONCLUSIONS

A comparison of the contrast in an umbra of leading/single and trailing sunspots for the cycle 24 growth phase and maximum confirmed the main conclusions drawn in (Zagainova, 2011). Using the data from instruments with a high spatial resolution that were mounted on the SDO spacecraft, we showed that the contrast in the He II 304 line above an umbra of leading and single sunspots is smaller than that above an umbra of trailing sunspots. Both for leading/single and trailing sunspots, the umbra contrast in He II 304 on average weakly depends on umbra area. On the other hand, the results of this work concerning the sunspot contrast in the He II 304 line slightly differ from the results achieved previously in (Zagainova, 2011). Thus, according to the SDO data for cycle 24, the average contrast values in $\lambda 304 \text{ \AA}$ above an umbra of leading/single and trailing sunspots were larger than the values obtained based on an analysis of the SOHO/EIT data for cycle 23 by factors of ~ 3.6 and ~ 2.7 , respectively. The possible cause of this difference for two sunspot samples is related to the fact that our work analyzed sunspots registered during the cycle 24 growth phase and maximum, whereas sunspots during the cycle 23 decline phase were analyzed in (Zagainova, 2011). It is known that cycle 24 is characterized by several specific features and even anomalies as compared to previous solar cycles. In addition to relatively small Wolf numbers, cycle 24 differs from other cycles by smaller values of the large-scale solar magnetic field, pronounced differences in the polar magnetic field polarity reversal, etc. (Akhmetov et al., 2014). Finally, cycle 24 followed a prolonged solar activity minimum, which could affect the cycle characteristics. Certainly, one more possible cause of the detected differences in the contrast values in the He II 304 line obtained in (Zagainova, 2001) and in the present work may be that the data used in these works was obtained using different instruments with different spatial resolutions, etc.

An analysis of the magnetic properties of magnetically connected leading–trailing sunspot pairs and single sunspots, obtained using the SDO/HMI vector

field measurements with a high spatial resolution, indicated that the magnetic properties agree with sunspot magnetic properties obtained based on the magnetic field calculations in a potential approximation. It was established that the minimal angle between the field direction and the positive (antisunward) normal to the solar surface at a point where the field was measured is smaller in leading sunspots than in trailing ones ($\alpha_{\min-\lambda s} < \alpha_{\min-\lambda s}$) in $\sim 84\%$ of the considered leading–trailing sunspot pairs. We also confirmed the conclusion made in our previous work (Zagainova et al., 2014) that a positive correlation exists between $\alpha_{\min-\lambda s}$ and $\alpha_{\min-\lambda s}$. At the same time, according to the SDO data, the average value of the minimal angle (α_{\min}) in leading and trailing sunspots is smaller than the values obtained based on the field calculations in a potential approximation by factors of ~ 2.4 and ~ 1.65 , respectively. According to the SDO data, it turned out that the average $\alpha_{\min-\lambda s}$ value is smaller than the average $\alpha_{\min-\lambda s}$ value by a factor of ~ 2.6 . According to (Zagainova et al., 2014), this difference is a factor of ~ 1.8 . Our analysis of sunspot magnetic properties based on the SDO data also showed that α_{\min} is smaller in single sunspots with well-developed umbra and penumbra than in leading sunspots. We confirmed our previous conclusion that α_{\min} slightly increases for sunspots of both types with increasing umbra magnetic field and area.

Although $\alpha_{\min-\lambda s}$ is on average relatively small, it reached several tens of degrees in some sunspots. Large $\alpha_{\min-\lambda s}$ values were in many trailing sunspots. In our previous work (Zagainova et al., 2014), we explained that such large $\alpha_{\min-\lambda s}$ and $\alpha_{\min-\lambda s}$ angles originate because the inclination of the umbra magnetic tube axis with respect to the normal to the solar surface is considerable. In this case the inclination of magnetic field lines with respect to the magnetic tube axis can be insignificant. Such a sunspot model was considered, e.g., in (Kuklin, 1985). Nevertheless, the origin of large α_{\min} values in sunspots of two types is still a problem to be solved.

In this work we for the first time compared the dependences of the maximal and average values of magnetic induction on the umbra area separately for leading and trailing sunspots. The main results of our analysis of these dependences can be formulated as follows.

1. Neither maximal nor average magnetic field values vanish when the area decreases to very small values.

2. In all cases the magnetic field in leading and single sunspots is larger than in trailing ones.

3. Our approximation gives the threshold area values, when the $B_{\max}(S)$ and $\langle B \rangle(S)$ curves start saturating: ≈ 25 and ≈ 10 MSH for leading and trailing sunspots, respectively. This corresponds to umbra radii of 5000 and 3100 km. The values obtained by us generally agree with the estimates made by Solov'ev and Kirichek (2014) and confirm the concept of a "shallow" sunspot developed by these researchers. At such an interpretation, our data indicate that trailing sunspots are possibly shallower formations.

A new our achievement is that we compared α_{\min} with the contrast in the 304 Å line above an umbra (C_{304}). It turned out that the C_{304} value increases for leading and trailing sunspots with decreasing α_{\min} (for single sunspots, this dependence is almost imperceptible since the sample of such sunspots is specific). This result possibly reflects an increase in the height of the plasma column above an umbra, which contributes to the emission registered in $\lambda 304$ Å when α_{\min} decreases. It is interesting that a negative correlation was also obtained for the dependence of the C_{304-ls}/C_{304-fs} ratio on $\alpha_{\min-ls}/\alpha_{\min-fs}$: when the latter ratio increases, the former ratio decreases. This reflects a different character of the $C_{304-ls}(\alpha_{\min-ls})$ and $C_{304-fs}(\alpha_{\min-fs})$ dependences.

The dependence of the sunspot contrast in $\lambda 304$ Å on the magnetic field maximum in an umbra (B_{\max}) is one more new result achieved in our work. It turned out that C_{304-ls} and C_{304-fs} remain on average unchanged when B_{\max} increases.

ACKNOWLEDGMENTS

We are grateful to the SOLIS, SDO/HMI, and SDO/AIA teams for the opportunity to use the data of these instruments without restriction. We thank G.V. Rudenko for the presented program that was used to select magnetically connected sunspot pairs.

This work was partially supported by the Russian Foundation for Basic Research, project no. 14-02-003-8.

REFERENCES

- Akhtemov, Z.S., Andreeva, O.A., Rudenko, G.V., Stepanian, N.N., and Fainstein, V.G., Temporal variations in the large-scale magnetic field of the solar atmosphere at heights from the photosphere to the source surface, *Bull. Crimean Astrophys. Observatory*, 2014, vol. 110, pp. 108–118.
- Antalova, A., The relation of the sunspot magnetic field and penumbra–umbra radius ratio, *Astron. Inst. Czechosl. Bull.*, 1991, vol. 42, pp. 316–320.
- Baranov, A.V., Magnetic fields of small sunspots, *Astron. Tsirk.*, 1974, vol. 847, p. 5.
- Beckers, J.M. and Schroter, E.H., The intensity, velocity and magnetic structure of a sunspot region. I: Observational technique; properties of magnetic knots, *Sol. Phys.*, 1968, vol. 4, no. 2, pp. 142–164.
- Bray, R. and Loughed, R., *Sunspots*, London: Chapman and Hall, 1964.
- Bumba, V., Magnetic fields in small and young sunspots, *Sol. Phys.*, 1967, vol. 1, nos. 3–4, pp. 371–376.
- Harvey, J., Solar magnetic fields—small scale, *Publ. Astron. Soc. Pac.*, 1971, vol. 83, no. 495, pp. 539–549.
- Harvey, J. and Livingston, W., Magnetograph measurements with temperature-sensitive lines, *Sol. Phys.*, 1969, vol. 10, no. 2, pp. 283–293.
- Houtgast, J. and Sluiter, A.Van., Statistical investigations concerning the magnetic fields of sunspots. I, *Bull. Astron. Inst. Netherlands*, 1948, vol. 10, pp. 325–333.
- Jin, C.L., Qu, Z.Q., Xu, C.L., Jhang, X.Y., and Sun, M.G., The relationships of sunspot magnetic field strength with sunspot area, umbral area and penumbra–umbra radius ratio, *Astrophys. Space Sci.*, 2006, vol. 306, nos. 1–2, pp. 23–27.
- Kuklin, G.V., East–west asymmetry of the Wilson effect, *Issled. Geomagn. Aeron. Fiz. Solnisa*, 1985, vol. 73, p. 52.
- Lemen, J.R., Title, A.M., Akin, D.J., et al., The atmospheric imaging assembly (AIA) on the solar dynamics observatory (SDO), *Sol. Phys.*, 2012, vol. 275, nos. 1–2, pp. 17–40.
- Livingston, W. and Harvey, J., Observational evidence for quantization in photospheric magnetic flux, *Sol. Phys.*, 1969, vol. 10, pp. 294–296.
- Livshits, M.A., Constancy of $\tau / 10830$ in plages and helium emission in a shortwave-radiation field, *Astron. Rep.*, 1975, vol. 52, p. 970–974.
- Maltby, P., Continuum observations and empirical models of the thermal structure of sunspots, *Proc. NATO Advanced Research Workshop on the Theory of Sunspots*, Cambridge, 1992, pp. 103–120.
- Nikol'skaya, K.I., He I excitation in chromospheric spicules, *Astron. Rep.*, 1966, vol. 43, p. 936.
- Obridko, V.N., *Solnechnye pyatna* (Sunspots), Moscow: Nauka, 1985.
- Pipin, V.V. and Kosovichev, A.G., The subsurface-shear-shaped solar $\alpha\Omega$ dynamo, *Astrophys. J.*, 2011, vol. 727, no. 2, pp. 1–4.
- Pozhalova, Zh.A., The study of selected helium lines in the solar spectrum, *Astron. Rep.*, 1988, vol. 65, pp. 1037–1046.
- Ringnes, T.B. and Jensen, E., On the relation between magnetic fields of sunspots in the interval 1917–56, *Astrophys. Norvegica*, 1960, vol. 7, no. 4, pp. 99–121.

- Rudenko, G.V., Extrapolation of the solar magnetic field within the potential-field approximation from full-disk magnetograms, *Sol. Phys.*, 2001, vol. 198, no. 1, pp. 5–30.
- Sheeley, N.R., Measurements of solar magnetic fields, *Astrophys. J.*, 1966, vol. 144, pp. 723–732.
- Sheeley, N.R., Observations of small-scale solar magnetic fields, *Sol. Phys.*, 1967, vol. 1, pp. 171–179.
- Sobotka, M., Semi-empirical models of sunspots in various phases of evolution, *Contrib. Astron. Obs. Skalnaté Pleso*, 1986, vol. 15, pp. 315–318.
- Solov'ev, A. and Kirichek, E., Basic properties of sunspots: Equilibrium, stability and long-term eigen oscillations, *Astrophys. Space Sci.*, 2014, vol. 352, no. 1, pp. 23–42.
- Stenflo, J.O., Magnetic-field structure of the photospheric network, *Sol. Phys.*, 1973, vol. 32, no. 1, pp. 41–63.
- Steshenko, N.V., Magnetic field of small sunspots and pores, *Bull. Crimean Astrophys. Observatory*, 1967, vol. 37, pp. 21–26.
- Vitinsky, Yu.I., Kopetsky, M., and Kuklin, G.V., *Statistika pyatnoobrazovatel'noi deyatel'nosti Solntsa* (Sunspot Formation Activity Statistics), Moscow: Nauka, 1986.
- Zagainova, Yu.S., He II $\lambda 304$ emission above sunspot umbrae, *Astron. Rep.*, 2011, vol. 55, no. 2, pp. 159–162.
- Zagainova, Yu.S., Fainshtein, V.G., Rudenko, G.V., and Obridko, V.N., Comparative analysis of magnetic field properties in leading and trailing sunspots, *Astron. Rep.*, 2014, no. 9, pp. 19–27.

Translated by Yu. Safronov